

Removal of Methyl Tertiary-Butyl Ether via ZnO-AgCl Nanocomposite Photocatalyst

Pengcheng Liu^{a*}, Zhenhua Xu^a, Xiao Ma^a, Zixuan Peng^a, Mingyue Xiao^a, Yuhao Sui^a

^aSchool of Energy Resources, China University of Geosciences, Beijing, 100083, China

Received: January 3, 2016; Revised: March 3, 2016; Accepted: April 4, 2016

ZnO-AgCl nanocomposites with different mass ratios were synthesized via a one-pot wet chemical method. The synthesized nanocomposites were characterized by SEM, XRD and photoluminescence spectroscopy. The ZnO-AgCl nanocomposites exhibited a significant enhancement of photocatalytic activity towards degradation of methyl tertiary butyl ether in aqueous solution due to the effective carrier separation performance. In addition, the proposed ZnO-AgCl also exhibited an excellent photostability.

Keywords: ZnO, AgCl; Methyl tertiary butyl ether; Photocatalysis, Photostability

Introduction

Methyl tertiary-butyl ether (MTBE) has received a very high attention over the last decade due to its widespread detection in indoor environments^{1,2}. MTBE is used as an additive of oxygen added to gasoline in order to elevate the octane number, combustion improvement, and reduce CO₂ production. However, MTBE has been recognized as a prevalent and persistent groundwater and surface water pollutant. Acute toxicity levels of MTBE for rodent LD₅₀ and lethal air concentrations for rats (LC₅₀) were estimated to be 3.8–3.9 g/kg and 65–126 g/m³, respectively^{3,4}. However, the presence of MTBE in water is mainly responsible for taste and odor related problems. Moreover, the International Agency of Research on Cancer (IARC) and the U.S. Environmental Protection Agency (EPA) classified MTBE as a health risk threat in 2000⁵. Therefore, removal of MTBE from water is an important issue.

So far, many methods have been studied for removing MTBE. Such as adsorption⁶, air stripping⁷, photocatalysis⁸, ozone treatment⁹, Fenton process¹⁰, high energy electron beam irradiation¹¹, cavitation¹², biodegradation¹³ and electrochemical oxidation¹⁴. Among them, designing suitable photocatalyst for MTBE degradation received a considerable attention due to its green approach, free sun energy and easy to scale-up. ZnO is a well-known *n*-type semiconductor with band gap energy of 3.37 eV, hence is considered as one of the best photocatalysts to deal with organic pollutant¹⁵⁻²¹. However, the photocatalytic activity of ZnO is still restricted by fast recombination of the photogenerated electron-hole pairs²²⁻²⁴. Many efforts have been made for extending the absorption range of ZnO, such as elements doping and metal-semiconductor heterostructure formation. Silver halides are widely recognized as photosensitive materials²⁵⁻³⁵. Recently, research showed that the Ag-AgCl supported metal oxide semiconductor has enhanced photocatalytic activity under visible or simulated solar light^{36,37}. Therefore, combining ZnO with silver halide is expected as an ideal photocatalyst for MTBE removal. Herein, we proposed a simple one-pot hydrothermal method for ZnO-AgCl nanocomposite formation. The photocatalytic activity of prepared ZnO-AgCl nanocomposite was tested. To

the best of our knowledge, this is the first report of using ZnO-AgCl nanocomposite for MTBE photodegradation.

Experimental

Materials

Zinc nitrate hexahydrate (Zn(NO₃)₂·6H₂O), ammonium hydroxide (28-30% NH₃ basis), silver nitrate (AgNO₃) and methyl tert-butyl ether (99%) were purchased from Sigma-Aldrich. All other chemicals used were analytical grade reagents without further purification. Milli-Q water (18.2 MΩ cm) was used throughout the experiments.

Preparation of ZnO-AgCl nanocomposite

Certain amount of zinc nitrate hexahydrate was dissolved in 50 mL of water. Then, 5 mL of ammonium hydroxide was added into the solution for 15 min stirring. Afterward, a certain amount of AgNO₃ solution (50 mM) was slowly added. After 30 min stirring, 5 mL of NaCl (0.5 M) was slowly added into the formed suspension. Then the suspension was refluxed at 110°C for 30 min. The precipitate was collected by centrifugation followed with water wash. The final product was obtained by calcination of the precipitate in a furnace at 150°C for 1 h (denoted as ZnO-AgCl-1, ZnO-AgCl-2 and ZnO-AgCl-3 for the mole ratios of Zn/Ag set as 3:1, 2:1 and 1:1, respectively).

Characterizations

The morphology and structure of the prepared samples were characterized using a field emission scanning electron microscope (FESEM, ZEISS SUPRA 40VP, Germany) and an X-ray diffractometer (D8 –Advance XRD, Bruker, Germany) with Cu Kα radiation, respectively. The Photoluminescence (PL) emission curves were obtained by a Fluorescence spectrophotometer (HORIBA Jobin Yvon Fluorolog-3-P, Japan)

Photodegradation of MTBE

Aqueous MTBE solutions were prepared by mixing MTBE with Milli-Q water. The pH of deionized water was adjusted to 7.0. For photodegradation, 200 ppb MTBE was prepared as a starting concentration.

*e-mail: liupengcheng8883@sohu.com

In a typical photodegradation experiment, 40 mg of photocatalyst was added into MTBE solution and kept under dark conditions for 30 min. After light irradiation, 2 mL of suspension was then taken out a certain period and the photocatalyst was separated by centrifugation. The concentration of MTBE was detected by GC-FID analysis³⁸. For comparison purpose, nano-size ZnO was synthesized using a similar method for ZnO-AgCl preparation except adding AgNO₃. P25 (commercial TiO₂ photocatalyst, containing both anatase and rutile phase of TiO₂) was also purchased and used as control group.

Results and Discussion

Characterization of ZnO-AgCl nanocomposite

Fig. 1 shows the SEM images of ZnO-AgCl-1 and ZnO-AgCl-3. As can be seen, the ZnO particles present a rod structure in the ZnO-AgCl nanocomposite with length varying from 30-200 nm. AgCl sphere are attached to the ZnO particles with a diameter of 180 nm. The attachment of the ZnO rods on the AgCl surface can be clearly absorbed.

The formation of ZnO and AgCl nanoparticles should be independent during the chemical reduction process. However, the high temperature reflux condition could produce diffusion-limited-aggregation process, which involves cluster growth by the adhesion of a particle to a seed on contact and growing surface after the reduction^{35,39}. It also can be seen that the size of ZnO particles slightly decrease after the mole ratio of Ag increases in the preparation stage. The morphology of ZnO-AgCl-2 (not present) is similar to that of ZnO-AgCl-1 while the ZnO-AgCl-3 shows a much higher content of AgCl particles than that of ZnO-AgCl-1.

Fig. 2A depicts the XRD patterns of the as-prepared ZnO-AgCl nanocomposite with different mass ratios of ZnO to AgCl. All XRD patterns exhibit peaks at 32.1°, 34.3°, 36.1°, 47.6°, 56.6°, 62.9°, 67.3°, 68.1°, 68.6°, 72.1° and 77.7°, which are related to the hexagonal ZnO (JCPDS 36-1451). Moreover, all samples also show the peaks at 26.1°, 45.3°, 54.3° and 56.7°, which corresponded to the cubic phase crystal structure of AgCl (JCPDS 31-1238). In addition, the AgCl peaks intensity increased along with

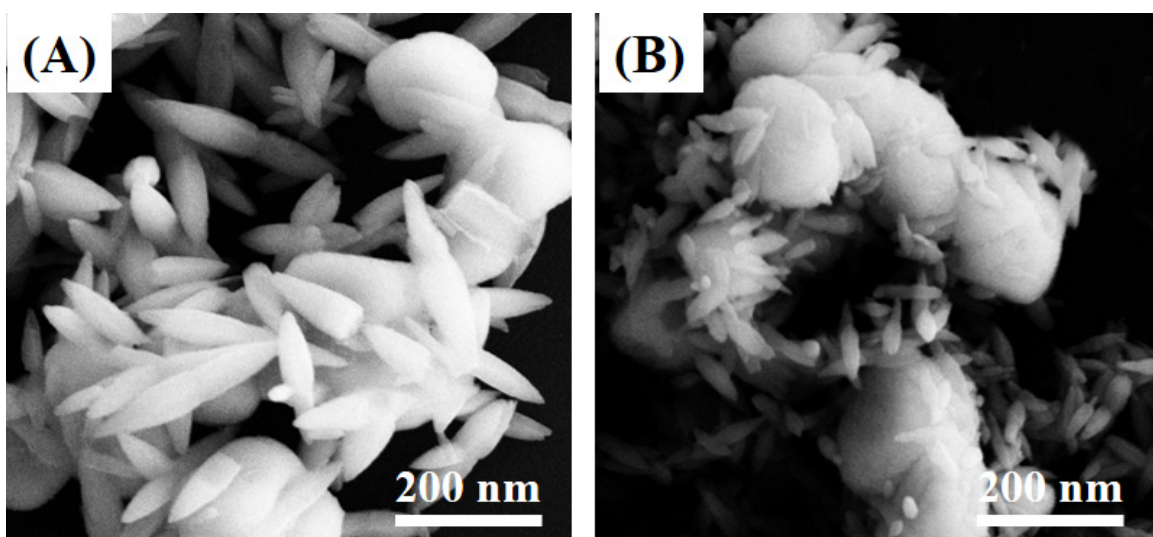


Fig. 1. SEM images of (A) ZnO-AgCl-1 and (B) ZnO-AgCl-3 nanocomposites.

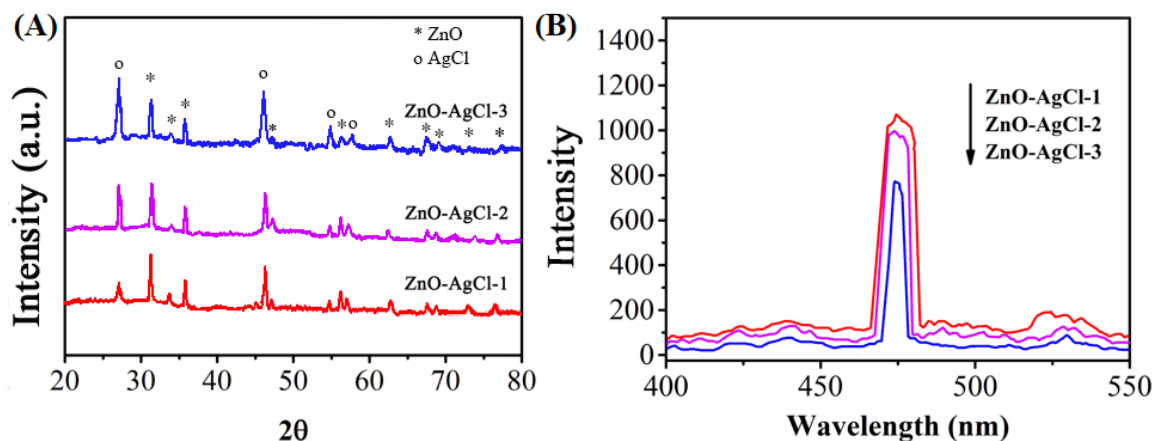


Fig. 2. (A) XRD patterns and (B) PL spectra of ZnO-AgCl-1, ZnO-AgCl-2 and ZnO-AgCl-3 nanocomposite.

the AgCl ratio increasing, suggesting the increase in AgCl content in the nanocomposite.

Fig. 2B shows the PL spectra of ZnO-AgCl-1, ZnO-AgCl-2 and ZnO-AgCl-3. Three main emission bands are observed in the ZnO, which can be attributed to the recombination of photogenerated electron-hole pairs, impurities and structural defects, and oxygen/zinc interstitials, for peaks located at 433 nm, 474 nm and 522 nm, respectively^{40,41}. The PL intensities decreasing along with the content of AgCl increasing, synergistic effect between ZnO and AgCl nanoparticles, which effectively reduces the electron-hole pairs recombination and facilitates the charge carrier separation. Among all these samples, ZnO-AgCl-3 displays the lowest PL intensity, which may lead to the highest photocatalytic activity.

Photodegradation of MTBE by ZnO-AgCl nanocomposites

The photocatalytic activity of as-prepared ZnO-AgCl nanocomposites was investigated by photodegradation of MTBE. Fig. 3A shows the photodegradation profile using 40 mg ZnO-AgCl-1, ZnO-AgCl-2 and ZnO-AgCl-3 without light irradiation. Where C_0 and C are the initial concentration of MTBE and concentration after irradiation, respectively. It can be seen that the concentration of

MTBE did not show a significant decreasing. The slight decreasing can be attributed to the adsorption of MTBE by nanocomposite. Therefore, the results indicate ZnO-AgCl nanocomposite show no photocatalytic activity towards decomposition of MTBE without light irradiation.

We further studied the photocatalytic properties of ZnO-AgCl nanocomposite. Fig. 3B shows the photodegradation profile using 40 mg ZnO-AgCl-1, ZnO-AgCl-2 and ZnO-AgCl-3 under visible light irradiation. It can be clearly seen that three photocatalysts show positive degradation performance toward MTBE. After 120 min visible irradiation, ZnO-AgCl-1, ZnO-AgCl-2 and ZnO-AgCl-3 nanocomposites can remove 62.1%, 92.3% and 77.11% of MTBE from water, respectively. The results did not match to our prediction from PL results. The photocatalytic activity of the ZnO-AgCl-2 showed a higher performance than that of the ZnO-AgCl-3, which could ascribe the sufficient amount of ZnO in the nanocomposite. Therefore, the ratio between ZnO and AgCl is very important factor in the photodegradation performance of ZnO-AgCl nanocomposite. The possible mechanistic pathway of the catalysts for photocatalytic degradation of MTBE is proposed as follows: under light irradiation, photogenerated electron-hole pairs ($e_{cb}^- - h_{vb}^+$) were formed in ZnO rods. Then, the h_{vb}^+ could react with AgCl to form Ag^+ and

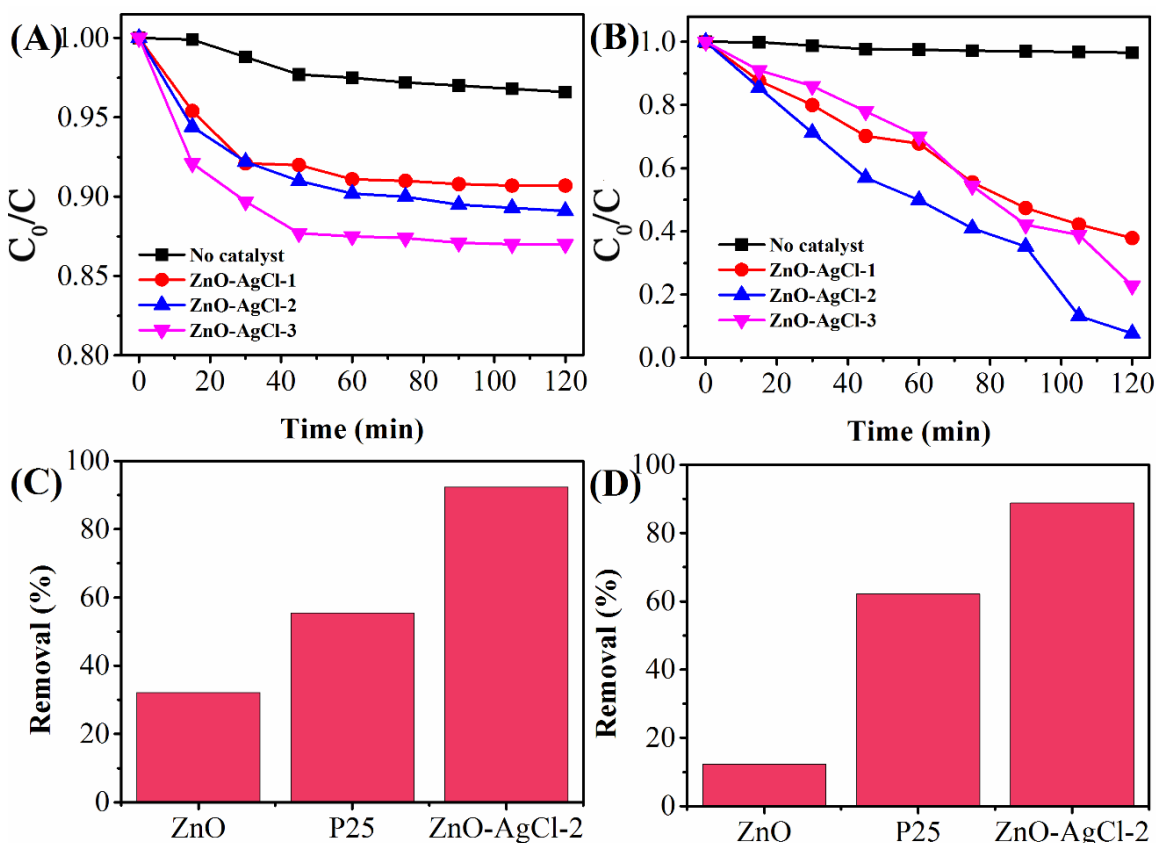


Fig. 3. (A) Degradation of MTBE over ZnO-AgCl-1, ZnO-AgCl-2 and ZnO-AgCl-3 without light irradiation. (B) Photodegradation of MTBE over ZnO-AgCl-1, ZnO-AgCl-2 and ZnO-AgCl-3. (C) MTBE removal rate using ZnO-AgCl-2, P25 and nano-ZnO under visible light irradiation. (D) MTBE removal rate using ZnO-AgCl-2, P25 and nano-ZnO under UV light irradiation.

Cl^0 . A part of h_{vb}^+ generated by ZnO reacted with OH^- to form $\bullet OH$. The Cl^0 and $\bullet OH$ could react with the MTBE pollutant. Therefore, although the ZnO-AgCl-3 showed a best electron-hole pairs recombination suppression performance, the lack of ZnO to produce the h_{vb}^+ restricted its photocatalytic activity. In order to evaluate the enhancement of nanocomposite, we also compared ZnO-AgCl-2 with nano-ZnO and commercial photocatalyst P25 (TiO_2 , rutile: anatase = 85: 15). Fig. 3C depicts the removal rate of three photocatalysts using the same conditions. As can be seen that, the removal efficiency order is ZnO-AgCl-2>P25>nano-ZnO. Therefore, our proposed ZnO-AgCl nanocomposite exhibits a clear enhancement towards photodegradation of MTBE.

Besides the visible light irradiation, we also tested the photodegradation performance of ZnO, ZnO-AgCl-2 nanocomposites and P25 under UV light irradiation. Fig. 3D displays the removal rate of MTBE using different photocatalysts after 60 mins UV light irradiation. It can be seen that the ZnO-AgCl-2 still exhibits best performance among the photocatalysts, indicating the ZnO-AgCl nanocomposite can be used as a photocatalyst under both UV light and visible light conditions.

The effects of photocatalyst loading were investigated at 10 mg, 20 mg, 30 mg, 40 mg, 50 mg and 60 mg of ZnO-AgCl-2 nanocomposite. As shown in Fig. 4A, all experiments showed clear degradation of MTBE. When insufficient amount of ZnO-AgCl-2 nanocomposite was added into MTBE solution, the low removal rate could be the result of limited production of OH^- caused by the inadequate conversion from light energy to chemical energy⁴². This can be evidenced by the enhancement of removal rate after increase in amount of ZnO-AgCl-2 nanocomposite. On the other hand, at a high concentration of ZnO-AgCl-2 nanocomposite, aggregation of photocatalyst is causing a decrease in the number of surface active sites and an increase in opacity and light scattering leads to a decrease in the transmission of irradiation through the sample⁴³. Therefore, 40 mg ZnO-AgCl-2 nanocomposite was used in this study.

The effect of pH on the photodegradation was also studied. As shown in Fig. 4B, the pH condition can apply a significant role in the photodegradation results due to the photocatalytic destruction mechanism in different pHs has different activation energies⁴⁴. At acid condition, the photocatalyst is protonated and became positively charged,

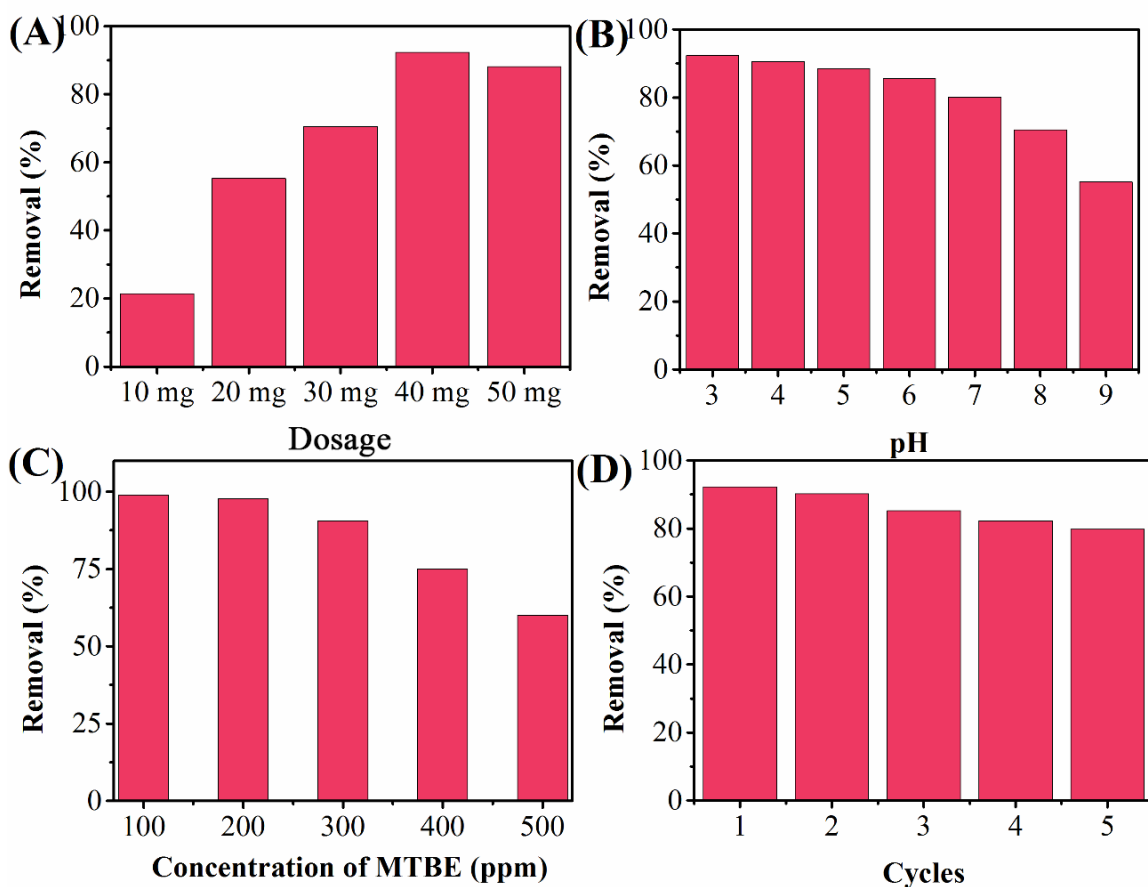


Fig. 4. (A) Effect of ZnO-AgCl-2 dosage on photodegradation efficiency of MTBE. (B) Effect of pH on photodegradation efficiency of MTBE. (C) Effect of concentration of MTBE on photodegradation efficiency of MTBE. (D) Reusability of ZnO-AgCl-2.

which is more favorable for the electron to move from the valance band to the conduction band of the semiconductor particle. Similar phenomenon was observed by other researchers⁴⁵⁻⁴⁶. Therefore, pH 3 is selected for optimum condition.

Fig. 4C shows the effect of initial concentration of MTBE on the photodegradation process. It can be seen that the higher initial MTBE concentration could lead to low final removal rate. This is caused not simply by the increase in amount of target molecules but the results are also influenced by suppression of OH⁻ radicals formation as a consequence of poisoning the catalyst surface by pollutant ions⁴⁷.

The stability of photocatalyst in photocatalytic reaction is an important factor in the practical applications. Therefore, the reusability of the ZnO-AgCl-2 nanocomposite was tested by 5 photodegradation cycles. As shown in Fig. 4D, the ZnO-AgCl-2 nanocomposite remain more than 80% of photodegradation performance in the 5th cycle of photodegradation, indicating that the proposed photocatalyst owing an excellent stability.

Reference

- Belpoggi F, Sofritti M, Maltoni C. Methyl-tertiary-butyl ether (MTBE)-a gasoline additive-causes testicular and lympho haematopoietic cancers in rats. *Toxicology and Industrial Health*. 1995;11(2):119-149.
- Smith AE, Hristova K, Wood I, Mackay DM, Lory E, Lorenzana D, et al. Comparison of biostimulation versus bioaugmentation with bacterial strain PM1 for treatment of groundwater contaminated with methyl tertiary butyl ether (MTBE). *Environmental Health Perspectives*. 2005;3113(3):317-322. <http://dx.doi.org/10.1289/ehp.6939>
- Kolb A, Püttmann W. Methyl tert-butyl ether (MTBE) in snow samples in Germany. *Atmospheric Environment*. 2006;40(1):76-86. <http://dx.doi.org/10.1016/j.atmosenv.2005.09.016>
- Kolb A, Püttmann W. Methyl tert-butyl ether (MTBE) in finished drinking water in Germany. *Environmental Pollution*. 2006;140(2):294-303. <http://dx.doi.org/10.1016/j.envpol.2005.07.008>
- Davis JM, Farland WH. The paradoxes of MTBE. *Toxicological Sciences*. 2001;61(2):211-217.
- Abu-Lail L, Bergendahl JA, Thompson RW. Adsorption of methyl tertiary butyl ether on granular zeolites: batch and column studies. *Journal of Hazardous Materials*. 2010;178(1):363-369. <http://dx.doi.org/10.1016/j.jhazmat.2010.01.088>
- Shih T, Wangpaichitr M, Suffet M. Performance and cost evaluations of synthetic resin technology for the removal of methyl tert-butyl ether from drinking water. *Journal of Environmental Engineering*. 2005;131(3):450-460. [http://dx.doi.org/10.1061/\(ASCE\)0733-9372\(2005\)131:3\(450\)](http://dx.doi.org/10.1061/(ASCE)0733-9372(2005)131:3(450))
- Mrowetz M, Pirola C, Selli E. Degradation of organic water pollutants through sonophotocatalysis in the presence of TiO₂. *Ultrasonics Sonochemistry*. 2003;10(4):247-254. [http://dx.doi.org/10.1016/S1350-4177\(03\)00090-7](http://dx.doi.org/10.1016/S1350-4177(03)00090-7)
- Patterson CL, Cadena F, Sinha R, Ngo-Kidd DK, Ghassemi A, Radha Krishnan E. Field treatment of MTBE-contaminated groundwater using ozone/UV oxidation. *Groundwater Monit. Rem.* 2013;33(2):44-52. <http://dx.doi.org/10.1111/j.1745-6592.2012.01418.x>
- Gonzalez-Olmos R, Roland U, Toufar H, Kopinke FD, Georgi A. Fe-zeolites as catalysts for chemical oxidation of MTBE in

Conclusion

In this study, a facile one-pot hydrothermal approach has been used to synthesize ZnO-AgCl nanocomposites, and their corresponding photocatalytic performance under visible irradiation was investigated. The results on MTBE photodegradation indicated that the as-prepared ZnO-AgCl nanocomposites have a superior photocatalytic activity than bare ZnO and P25. Additionally, the reusability test showed that the ZnO-AgCl photocatalyst remained more than 80% photocatalytic activity in the fifth cycle, which made it high promising for practical applications such as waste water purification.

Acknowledgements

This research was conducted with financial support from the Science and Technology Special Funds of China for 2016ZX05015 and 2016ZX05016. The authors would like to thank the State Key Laboratory of Enhanced Oil Recovery Research, Institute of Exploration and Development, PetroChina.

- water with H₂O₂. *Applied Catalysis B: Environmental*. 2009;89(3-4):356-364. <http://dx.doi.org/10.1016/j.apcatb.2008.12.014>
- Basfar AA, Khan HM, Al-Shahrani AA, Cooper WJ. Radiation induced decomposition of methyl tert-butyl ether in water in presence of chloroform: kinetic modelling. *Water Research*. 2005;39(10):2085-2095. <http://dx.doi.org/10.1016/j.watres.2005.02.019>
- Kim DK, O'Shea KE, Cooper WJ. Mechanistic considerations for the degradation of methyl tert-butyl ether (MTBE) by sonolysis: effect of argon vs. oxygen saturated solutions. *Ultrasonics Sonochemistry*. 2012;19(4):959-968. <http://dx.doi.org/10.1016/j.ulsonch.2011.12.003>
- Shah NW, Thornton SF, Bottrell SH, Spence MJ. Biodegradation potential of MTBE in a fractured chalk aquifer under aerobic conditions in long-term uncontaminated and contaminated aquifer microcosms. *Journal of Contaminant Hydrology*. 2009;103(3):119-133. <http://dx.doi.org/10.1016/j.jconhyd.2008.09.022>
- Wu TN. Electrochemical removal of MTBE from water using the iridium dioxide coated electrode. *Separation and Purification Technology*. 2011;79(2):216-220. <http://dx.doi.org/10.1016/j.seppur.2011.02.008>
- Khani A, Sohrabi MR, Khosravi M, Davallo M. Enhancing purification of an azo dye solution in nanosized zero-valent iron-ZnO photocatalyst system using subsequent semibatch packed-bed reactor. *Turkish Journal Engineering Environmental Sciences*. 2013;37(1):91-99. <http://dx.doi.org/10.3906/muh-1201-6>
- Zhang C, Zhang J, Su Y, Xu M, Yang Z, Zhang Y. ZnO nanowire/reduced graphene oxide nanocomposites for significantly enhanced photocatalytic degradation of Rhodamine 6G. *Physica E*. 2014;56:251-255. <http://dx.doi.org/10.1016/j.physe.2013.09.020>
- Zheng Y, Fu L, Wang A, Peng F, Yang J, Han F. One-pot hydrothermal preparation of SnO₂-ZnO nanohybrids for simultaneous electrochemical detection of catechol and hydroquinone. *Sensor Letters*. 2015;13(10):878-882. <http://dx.doi.org/10.1166/sl.2015.3543>
- Xu S, Fu L, Pham TS, Yu A, Han F, Chen L. Preparation of ZnO flower/reduced graphene oxide composite with enhanced photocatalytic performance under sunlight. *Ceramics*

- International*. 2015;41(3):4007-4013. <http://dx.doi.org/10.1016/j.ceramint.2014.11.086>
19. Fu L, Zheng Y, Wang A, Cai W, Deng B, Zhang Z. An electrochemical sensor based on reduced graphene oxide and ZnO nanorods-modified glassy carbon electrode for uric acid detection. *Arabian Journal for Science and Engineering*. 2016;41(1):135-141.
 20. Fu L, Lai G, Zhang H, Yu A. One-pot synthesis of multipod ZnO-Carbon nanotube-reduced graphene oxide composites with high performance in photocatalysis. *Journal of Nanoscience and Nanotechnology*. 2015;15(6):4325-4331. <http://dx.doi.org/10.1166/jnn.2015.9806>
 21. Fu L, Fu Z. Plectranthus amboinicus leaf extract assisted biosynthesis of ZnO nanoparticles and their photocatalytic activity. *Ceramics International*. 2015;41(2):2492-2496. <http://dx.doi.org/10.1016/j.ceramint.2014.10.069>
 22. Wang Q, Plylahan N, Shelke MV, Devarapalli RR, Li M, Subramanian P, Djenizian T, et al. Nanodiamond particles/reduced graphene oxide composites as efficient supercapacitor electrodes. *Carbon*. 2014;68:175-184. <http://dx.doi.org/10.1016/j.carbon.2013.10.077>
 23. Wei A, Xiong L, Sun L, Liu Y, Li W, Lai W, et al. One-step electrochemical synthesis of a graphene-ZnO hybrid for improved photocatalytic activity. *Materials Research Bulletin*. 2013;48(8):2855-2860. <http://dx.doi.org/10.1016/j.materresbull.2013.04.012>
 24. Lamba R, Umar A, Mehta SK, Anderson WA, Kansal SK. Visible-light-driven photocatalytic properties of self-assembled cauliflower-like AgCl/ZnO hierarchical nanostructures. *Journal of Molecular Catalysis A*. 2015;408:189-201. <http://dx.doi.org/10.1016/j.molcata.2015.07.016>
 25. Xue B, Sun T, Wu JK, Mao F, Yang W. AgI/TiO₂ nanocomposites: Ultrasound-assisted preparation, visible-light induced photocatalytic degradation of methyl orange and antibacterial activity. *Ultrasonics Sonochemistry*. 2015;22:1-6. <http://dx.doi.org/10.1016/j.ulsonch.2014.04.021>
 26. Adhikari R, Gyawali G, Sekino T, Wohn Lee S. Microwave assisted hydrothermal synthesis of Ag/AgCl/WO₃ photocatalyst and its photocatalytic activity under simulated solar light. *Journal of Solid State Chemistry*. 2013;197:560-565. <http://dx.doi.org/10.1016/j.jssc.2012.08.012>
 27. Fu L, Wang A, Zheng Y, Cai W, Fu Z. Electrodeposition of Ag dendrites/AgCl hybrid film as a novel photodetector. *Materials Letters*. 2015;142:119-121. <http://dx.doi.org/10.1016/j.matlet.2014.12.001>
 28. Fu L, Fu Z. Plectranthus amboinicus leaf extract-assisted biosynthesis of ZnO nanoparticles and their photocatalytic activity. *Ceramics International*. 2015;41(2 Part A):2492-2496. <http://dx.doi.org/10.1016/j.ceramint.2014.10.069>
 29. Fu L, Cai W, Wang A, Zheng Y. Photocatalytic hydrogenation of nitrobenzene to aniline over tungsten oxide-silver nanowires. *Materials Letters*. 2015;142:201-203. <http://dx.doi.org/10.1016/j.matlet.2014.12.021>
 30. Shekofteh-Gohari M, Habibi-Yangjeh A. Novel magnetically separable Fe₃O₄@ZnO/AgCl nanocomposites with highly enhanced photocatalytic activities under visible-light irradiation. *Separation and Purification Technology*. 2015;147:194-202. <http://dx.doi.org/10.1016/j.seppur.2015.04.034>
 31. Naghizadeh-Alamdari S, Habibi-Yangjeh A, Pirhashemi M. One-pot ultrasonic-assisted method for preparation of Ag/AgCl sensitized ZnO nanostructures as visible-light-driven photocatalysts. *Solid State Sciences*. 2015;40:111-120. <http://dx.doi.org/10.1016/j.solidstatesciences.2015.01.007>
 32. Pirhashemi M, Habibi-Yangjeh A. Preparation of AgCl-ZnO nanocomposites as highly efficient visible-light photocatalysts in water by one-pot refluxing method. *Journal of Alloys and Compounds*. 2014; 601:1-8. <http://dx.doi.org/10.1016/j.jallcom.2014.02.111>
 33. Li W, Hua F, Yue J, Li J. Ag@AgCl plasmon-induced sensitized ZnO particle for high-efficiency photocatalytic property under visible light. *Applied Surface Science*. 2013;285(Part B):490-497. <http://dx.doi.org/10.1016/j.apsusc.2013.08.082>
 34. Fu L, Yong J, Lai G, Tamanna T, Notley S, Yu A. Nanocomposite coating of multilayered carbon nanotube-titania. *Materials and Manufacturing Processes*. 2014;29(9):1030-1036. <http://doi.org/10.1080/10426914.2014.880465>
 35. Fu L, Lai G, Mahon PJ, Wang J, Zhu D, Jia B, Malherbe F, Yu A. Carbon nanotube and graphene oxide directed electrochemical synthesis of silver dendrites. *RSC Advances*. 2014; 4:39645-39650. <http://dx.doi.org/10.1039/C4RA06156J>
 36. Fu L, Wang A, Zheng Y, Cai W, Fu Z. Electrodeposition of Ag dendrites/AgCl Hybrid film as a novel photodetector. *Materials Letters*. 2015;142(1):119-121. <http://dx.doi.org/10.1016/j.matlet.2014.12.001>
 37. Fu L, Lai G, Jia B, Yu A. Preparation and electrocatalytic properties of polydopamine functionalized reduced graphene oxide-silver nanocomposites. *Electrocatalysis*. 2015;6(1):72-76. <http://dx.doi.org/10.1007/s12678-014-0219-9>
 38. Siddiqui MN, Gondal MA. Nanocatalyst support of laser-induced photocatalytic degradation of MTBE. *Journal of Environmental Science and Health A*. 2014; 49(1):52-58. <http://dx.doi.org/10.1080/10934529.2013.824298>
 39. Fu L, Tamanna T, Hu WJ, Yu A. Chemical preparation and applications of silver dendrites. *Chemical Papers*. 2014;68(10):1283-1297. <http://dx.doi.org/10.2478/s11696-014-0582-2>
 40. Tien HN, Khoa NT, Hahn SH, Chung JS, Shin EW, Hur SH. One-pot synthesis of a reduced graphene oxide-zinc oxide sphere composite and its use as a visible light photocatalyst. *Chemical Engineering Journal*. 2013;229:126-133. <http://dx.doi.org/10.1016/j.cej.2013.05.110>
 41. Matsuyama K, Mishima K, Kato T, Ohara K. Preparation of hollow ZnO microspheres using poly (methyl methacrylate) as a template with supercritical CO₂-ethanol solution. *Industrial Engineering Chemistry Research*. 2010;49(18):8510-8517. <http://dx.doi.org/10.1021/ie100551t>
 42. Nikazar M, Gorji LM, Shojae S, Keynejad K, Haghghaty A, Jalili F, Mirzahassemi A. Removal of methyl tertiary-butyl ether (MTBE) from aqueous solution using sunlight and nano TiO₂. *Energy Sources Part A*. 2014;36(20):2305-2311. <http://doi.org/10.1080/15567036.2012.658140>
 43. Sohrabi M, Ghavami M. Photocatalytic degradation of Direct Red 23 dye using UV/TiO₂: Effect of operational parameters. *Journal of Hazardous Materials*. 2008;153(3):1235-1239. <http://dx.doi.org/10.1016/j.jhazmat.2007.09.114>
 44. Ghodbane H, Hamdaoui O, Vandamme J, Van Durme J, Vanraes P, Leys C, et al. Degradation of AB25 dye in liquid medium by atmospheric pressure non-thermal plasma and plasma combination with photocatalyst TiO₂. *Open Chemistry*. 2015;13(1):325-331. <http://dx.doi.org/10.1515/chem-2015-0040>
 45. Habib A, Ismail IM, Mahmood J, Ullah R. Photocatalytic decolorization of Brilliant Golden Yellow in TiO₂ and ZnO suspensions. *Journal of Saudi Chemical Society*. 2012;16(4):423-429. <http://dx.doi.org/10.1016/j.jscs.2011.02.013>
 46. Noguchi H, Nakajima A, Watanabe T, Hashimoto K. Design of a photocatalyst for bromate decomposition: Surface modification of TiO₂ by pseudo-boehmite. *Environmental Science & Technology*. 2003;37(1):153-157. <http://dx.doi.org/10.1021/es0258733>
 47. Rashed M, El-Amin A. Photocatalytic degradation of methyl orange in aqueous TiO₂ under different solar irradiation sources. *International Journal of Physical Science*. 2007;2(3):73-81.